NASA DEVELOP National Program
Idaho – Pocatello

Summer 2021

Southwest Water Resources

Monitoring Surface Water Extents of Remote Stock Ponds in the Southwestern United States Using Earth Observing Systems for Enhanced Water Resources Management

DEVELOP Technical Report

Final – August 12th, 2021

Rainey Aberle (Project Lead)
Rebecca Bernat
Michael Corley
Lukman Fashina
Kyle Paulekas

Advisors:
Seungbum Kim (NASA Jet Propulsion Laboratory Radar Remote Sensing)
Keith Weber (Idaho State University GIS Training and Research Center)

1. Abstract

Due to increasingly frequent and severe drought conditions in the southwestern US, land managers and livestock producers need to monitor stock ponds with increasing regularity. The ability to assess stock pond water levels with Earth observing satellite systems would enhance monitoring efforts of partners at the US Forest Service, Arizona Department of Game and Fish, and the Diablo Trust. This study employed Landsat 8 Operational Land Imager (OLI), Sentinel-1 C-band Synthetic Aperture Radar (C-SAR), and Sentinel-2 Multispectral Instrument (MSI) to monitor surface water extent for hundreds of critical stock ponds in Arizona. Using methods adapted from previously developed image processing workflows, this project conducted a time-series analysis to capture seasonal and interannual variations in surface water area between 2013 to 2021. In addition, end users can monitor the surface water extent of stock ponds through the developed Google Earth Engine software tool called Surface Water Identification and Forecasting Tool (SWIFT). SWIFT incorporates the Automated Water Extraction Index, Modified Normalized Difference Water Index, and Tasseled Cap-Wetness Index for optical imagery and the incidence angle, VV and VH polarization bands for Sentinel-1 imagery to detect small water bodies in the study area with an overall accuracy range of 88-93%. These tools will empower our partners to monitor the extents of water in their stock ponds remotely, enabling them to develop data-informed and sustainable management solutions for decades to come.

Key Terms

Stock ponds, water monitoring, livestock, remote sensing, Landsat 8, Sentinel-1, Sentinel-2, US Southwest

2. Introduction

2.1 Background Information

In the Southwestern United States, increasingly frequent drought conditions have become problematic for land and livestock managers. These drought conditions reduce precipitation and increase evaporation rates, which limit the ability of water to accumulate and remain as surface water. Stock ponds across the Southwestern US provide water to livestock and wildlife. Sufficient water supply is essential for maintaining quality animal health and production, especially species raised on pastures and rangelands like cattle, sheep, and goats. Arid ecosystems are particularly susceptible to climate change and climate variability (Archer and Predick, 2008). For example, environmental temperature, humidity, livestock diet and stage of growth all influence water intake (Meehan et al., 2021). Monitoring stock ponds is challenging due to their often-remote locations. Ranchers and land managers either relied on past occurrences or drove to assess ponds' water levels. Therefore, land managers and ranchers need a monitoring tool that is efficient, cost-effective, and reliable to decide appropriate livestock locations or make wildlife management decisions.

This study assessed variations in the extent of surface water bodies from March 2013 to August 2021 in the Coconino and Yavapai Counties in Northern Arizona. The stock ponds identified in this study are located on US Forest Service land (Figure 1). The landscape is characterized as a desert shrub, ponderosa pine, and sub-alpine fir forest. From 1971 to 2021, summer (June-August) temperatures averaged 71.7 ^{0}F and 76.8 ^{0}F in Coconino and Yavapai Counties, respectively (National Centers for Environmental Information [NCEI], 2021a; NCEI, 2021b); precipitation averaged 3.83 inches and 4.47 inches in Coconino and Yavapai Counties, respectively (NCEI, 2021c; and NCEI, 2021d).

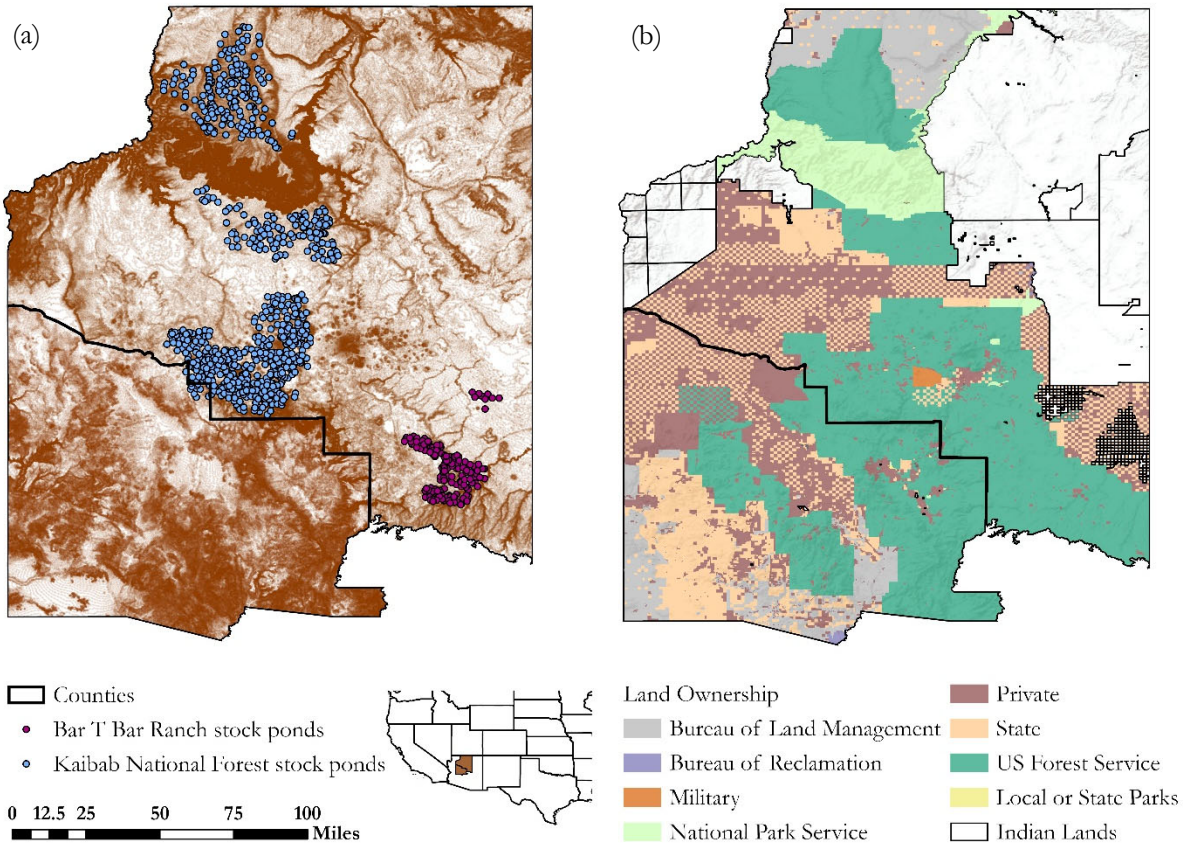

Figure 1. Maps of the study area, including a regional map of the US. Map (a) indicates stock pond point locations (blue and purple dots). Map (b) shows land ownership in Coconino (North) and Yavapai (South) Counties.

Previous research (Feyisa et. al., 2014; Fisher et al., 2016; Herndon et. al, 2020) has demonstrated the feasibility of Earth observations (EO) to detect surface water bodies. Some of these research studies have been conducted on small water body detection using EO, and notable among these is the work of Soti et al. (2009), where Landsat 8 Operational Land Imager (OLI) was utilized for the detection of ponds less than 0.27 acres in size by employing water detection indices. Based on the unique spectral pattern of water, identifying surface water from remote sensing data involves the use of indices with high accuracy in arid environments like the Modified Normalized Difference Water Index (MNDWI) and the Tasseled Cap-wetness index (TCW). TCW performs best in low-density vegetation because of its ability to identify moisture in vegetation (Baig et al., 2014). MNDWI enhances water body detection by increasing the rejection of land and flora features (Xu, 2006). The indices can establish a threshold value to delineate water body extent for accurate water body monitoring.

2.2 Project Partners & Objectives

This project was conducted in collaboration with US Forest Service (USFS), Rocky Mountain Research Station; USFS, Kaibab National Forest; Arizona Department of Game and Fish; and Diablo Trust. Partners previously relied exclusively on ground measurements to monitor stock pond fill levels, including some measurements using ground-based LiDAR instruments. For this project, partners were interested in employing NASA EO to more efficiently assess and forecast fill levels in regional stock ponds and tanks. Thus, we collaborated with the Rocky Mountain Research Center to create publicly available end products for future use by the Kaibab National Forest, Arizona Department of Game and Fish, and Diablo Trust.

Diablo Trust is a private organization which collaborates with ranchers and land managers who are focused on ensuring long-term economic, social and ecological sustainability of ranching in the US Southwest. Diablo Trust works collaboratively with USFS, Flying M Ranch, Bar T Bar Ranch, and Northern Arizona University to facilitate research about the protection and preservation of natural resources to further promote working lands in the West. Arizona Department of Game and Fish and USFS Range Management Program works with landowners and ranchers to manage agricultural land and water resources. Water resources management is a state prerogative, but constitutional powers are granted to USFS on federal lands (Abrams, 2010). Arizona Department of Game and Fish and cattle producers abide by state water law. Ranchers rely on precipitation and surface water runoff to replenish their ponds. To maintain cattle and water resources, land managers and ranchers rely heavily on site visits and measurements to evaluate the level of their ponds.

To address the goals for the project as communicated by the partners, our primary project objectives were to (1) determine the appropriate indices and EO products to employ for the classification of surface water extents, (2) create a time series map of automatically delineated regional surface water areal extents from March 2013 to August 2021, and (3) create an accessible tool for future surface water extent change detection that enables bi-weekly stock pond water availability. The detailed methods for completing each of these objectives are described below.

3. Methodology

3.1 Data Acquisition

3.1.1 Satellite Imagery

To identify stock ponds within the study area, we used optical imagery derived from Landsat 8 OLI and Sentinel-2 Multispectral Instrument (MSI), and radar imagery from Sentinel-1 C-Band Synthetic Aperture Radar (C-SAR), shown in Appendix A. We accessed all imagery through Google Earth Engine's (GEE) cloud-based resources to facilitate sharing end products with partners. Landsat 8, launched in 2013, orbits the Earth in a sun-synchronous orbit at an altitude of 705 km and with a repeat cycle of 16 days. The spectral bands of the Landsat 8 OLI surface reflectance product employed here are available at 30 m resolution. The European Space Agency (ESA) Sentinel-2 mission is comprised of two polar-orbiting satellites with a sun-synchronous orbit and a repeat cycle of 10 days (Copernicus, 2021). The spectral bands of the Sentinel-2 MSI are available at 10-20 m resolution. The ESA Sentinel-1 satellite mission is comprised of two satellites, A and B, which launched in 2014 and 2016, respectively. Each satellite completes a near-polar, sun-synchronous orbit with a combined repeat cycle of 6 days (Copernicus). The Sentinel-1 Ground Range Detected (GRD) products available through GEE have been pre-processed using the ESA Sentinel-1 Toolbox and are available at multiple spatial resolutions (10 m, 25 m, or 40 m) and four polarization bands.

3.1.2 Stock Pond Locations

Project partners provided more than 1000 known stock pond point locations within USFS and Bar T Bar Ranch jurisdictions (Figure 1). In addition, we used Maxar Imagery captured in the month of January 2018 available through Esri to digitize 1424 points, which were visually classified as "water" or "non-water." These digitized points were used both for training the classification model as well as the accuracy assessment, discussed in Sections 3.2 and 3.3 below.

3.2 Data Processing

This section describes the pre-processing, classification, post-processing, and accuracy assessment workflow for optical and radar imagery used to classify stock pond areal extent from March 2013 to August 2021. Figure 2 shows the team's step-by-step methodology in a flowchart.

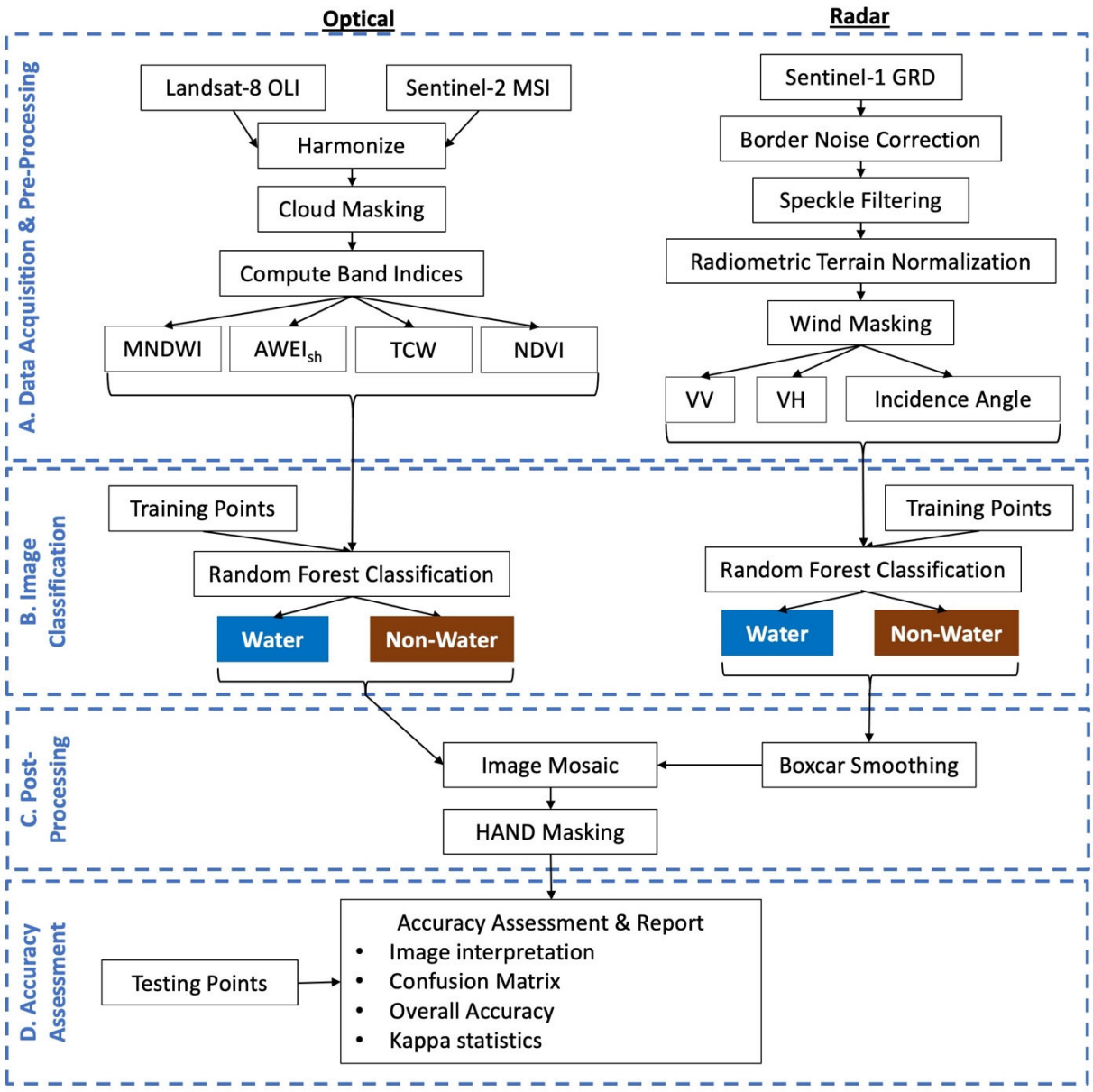

Figure 2. Flowchart showing the general image processing workflow applied in this study. A) Data Acquisition & Pre-processing for the Landsat 8 OLI, Sentinel-2 MSI, and Sentinel-1 GRD data products, resulting in Modified Normalized Difference Water Index (MNDWI), Automated Water Extraction Index, shadow-corrected (AWEIsh), Tasseled-Cap Wetness (TWC), and Normalized Difference Vegetation Index (NDVI) spectral band indices for the optical image collection, and analysis-ready data products for the radar image collection. B) Classification of water pixels using the training data as inputs. C) Post-processing steps including Smoothing of the Sentinel-1 classified collection using a Boxcar kernel smoothing algorithm and Image Mosaicking. D) Accuracy Assessment and Report of the resulting classified water bodies using the testing points.

3.2.1 Pre-Processing: Optical Imagery

To classify stock ponds using the complete collection of optical imagery, including Landsat 8 and Sentinel-2 surface reflectance products available in GEE, we first removed all images with a cloud cover greater than 10% as reported in the image metadata. To further remove the influence of cloud cover in the remaining

images in the collection, we then applied a cloud-masking algorithm using object segmentation techniques on the near-infrared, cirrus, and thermal bands in both Landsat 8 and Sentinel-2 imagery to detect clouds (Zhu and Woodstock, 2012; Zhu et al., 2015; Mishra et al., 2020). Next, we calculated several image band indices as shown in Table 1, which have been previously employed for efficient surface water detection in optical imagery (Feyisa et al., 2014; Nguyen et al., 2019; Fisher et al., 2016; Herndon et al., 2020). These indices include Automated Water Extraction Index, shadow-corrected (AWEIsh), Modified Normalized Difference Water Index (MNDWI), Tasseled-Cap Wetness (TCW), and Normalized Difference Vegetation Index (NDVI).

Table 1

Summary of band indices used for surface water detection in optical imagery, where ρ denotes the surface reflectance of each respective band.

Name	Equation	Bands Used					
		B	*G*	*R*	*NIR*	*SWIR1*	*SWIR2*
MNDWI	$(\rho_{Green} - \rho_{SWIR}) / (\rho_{Green} + \rho_{SWIR1})$		X			X	
$AWEI_{sh}$	$\rho_{Blue} + 2.5\rho_{Green} - 1.5(\rho_{NIR} + \rho_{SWIR1}) - 0.25\rho_{SWIR2}$		X		X	X	X
TCW	$0.1511(\rho_{Blue}) + 0.1973(\rho_{Green}) + 0.3283(\rho_{Red}) + 0.3407(\rho_{NIR}) - 0.7117(\rho_{SWIR1}) - 0.4559(\rho_{SWIR2})$	X	X	X	X	X	X
NDVI	$(\rho_{NIR} - \rho_{Red}) / (\rho_{NIR} + \rho_{Red})$			X	X		

3.2.2 Pre-Processing: Radar Imagery

To classify water bodies using Sentinel-1 C-SAR GRD collection, we first conducted the pre-processing workflow described by Mullissa et al. (2021), which includes publicly available scripts for image processing in GEE. The major steps of the workflow include border noise correction, speckle filtering, and radiometric terrain normalization of each image in the Sentinel-1 image collection. The resulting analysis-ready data are in gamma naught, as defined by Hoekman and Reiche (2015).

Although radar imagery is not affected by cloud cover, high wind speeds can impact surface roughness, particularly for bodies of water, which can lead to higher radar backscatter reaching the sensor (Alsdorf et al., 2007) and increased omission errors in classifying water bodies. Therefore, we applied a wind masking algorithm using wind observations near the time of image capture from the National Center for Environmental Prediction Climate Forecast System Version 2 6-hourly product (Saha et al., 2011) and previously published code from Gulácsi and Kovács (2020), which masks all pixels with a wind speed greater than 12 km/h near the time of image capture.

3.2.3 Classification

In order to classify pre-processed images as "water" or "non-water" areas, we employed a Random Forest Classification model for both the optical and radar image collections. To train the models before application to the image collection, we first visually classified 1424 points as "water" and "non-water" in Maxar imagery captured 27-30 January 2018, which we then overlaid onto all Landsat 8 and Sentinel-2 captured within one week of the Maxar imagery. We used the resulting spectral band indices and water property (i.e., "water" or "non-water") at 80% of the 1424 observed to train the Random Forest Classification Model. We set aside the remaining 20% of observed points for accuracy assessment of the classification model, described in Section 3.3.3 below. For optical imagery, the MNDWI, $AWEI_{sh}$, TCW, and NDVI bands were used as predictors. For radar imagery, the co-polarization (VV) and cross-polarization (VH) bands and the incidence angle were used as predictors. Following development of the classification models, we classified the complete image collection, resulting in a binary image collection of "water" (0) and "non-water" (1) points.

3.2.4 Post-Processing

The classification of Sentinel-1 C-SAR imagery relies on the assumption that smooth water surfaces produce low backscatter returns to the radar antenna, contrasting with the high backscatter of soil and vegetation surfaces (Ovakoglou et al., 2021). Upon visual inspection of the classified Sentinel-1 image collection, we found substantial noise in a variety of landscape settings likely due to surface roughness variations with some identified non-water pixels being classified as water. To mitigate these misclassifications, we applied a square-shaped Boolean kernel convolution to smooth the imagery using a window of five pixels, resulting in a single-band image with pixel values ranging from 0 to 1. Following visual analyses to identify the optimal threshold value for water detection, pixels with a classification value greater than or equal to 0.97 following the smoothing convolution were classified as water. To simplify data processing, as well as to increase the geographic and temporal coverage of surface water extent observations, we then created image mosaics for all classified images captured within the same week. Where images overlapped, we computed the median classification value (between 0 and 1) at each pixel, where a value of 1 represents water pixels.

Next, to minimize the anomalies associated with topography for Sentinel-1 C-SAR and snow cover or high-elevation features in optical imagery, we filtered out all pixels in the image mosaic collection with a Height Above Nearest Drainage (HAND) index above 10 m. HAND is a terrain index that normalizes local topography according to the relative heights found along with the drainage network in flood, soil moisture, and water availability mapping applications (Nobre et al., 2011; Hamdani and Baali, 2019; Garousi-Nejad et al., 2019; Bioresita et al., 2018). The HAND index has been used to define hydrologically consistent catchments (Nobre et al., 2011) and to filter out backscatter anomalies due to topography to reduce commission errors (Bioresita et al., 2018). To employ this technique, we used the HAND band from MERIT Hydro (Yamazaki et al., 2019), which provides high-resolution raster hydrography maps available through GEE. Because all water major bodies and identified stock ponds in the study area present a HAND index of less than 10 m, pixels with a HAND index above 10 m were set to no-data values.

3.3 Data Analysis

Finally, to create the time series of historical surface water extents, we computed the total surface area of water for each weekly classified image mosaic in both the entire study area and for each grazing allotment in Arizona. As a supplement to the time series maps of surface water extents, we designed an accessible tool using the GEE graphical user interface (GUI) capability called the Surface Water Identification and Forecasting Tool (SWIFT). This tool enables users to select a grazing allotment in the Southwest US and to view the total surface water extent for the most recent satellite imagery, as well as a classified image, true color image, and the historical time series of surface water extents within the grazing allotment. Data can be exported for further analyses external to SWIFT. We provided partners with a tutorial with instructions and primary steps for accessing data through the tool. SWIFT will allow partners to: (1) analyze both spatial and temporal trends in surface water extents throughout grazing allotments in the Southwest US, (2) compute the near-real time (within 1-2 weeks of the date of access) water levels in grazing allotments, and (3) compile water extent forecasting resources towards developing adaptive land, livestock, and wildlife management strategies in years to come. To assess the classification accuracy for both the optical and radar Random Forest Classification models, we computed the overall accuracy, confusion matrix, and kappa statistics for the ~20% of the 1424 observed points (Figure 3) set aside for testing.

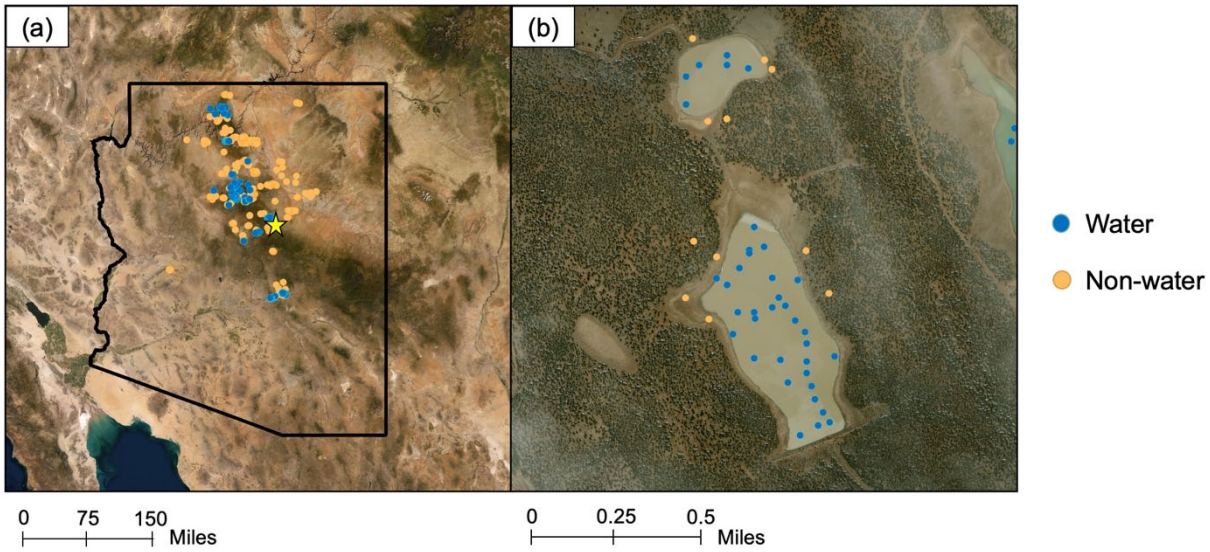

Figure 3. (a) Map of all digitized points used for training the classification models and the accuracy assessment. Blue points represent "water" and orange points represent "non-water" points. The yellow start represents the zoomed in region shown in panel (b).

4. Results & Discussion

4.1 Analysis of Results

4.1.1 Surface Water Identification and Forecasting Tool (SWIFT)

The method used to create the historical time series was also used to develop an accessible tool using the GEE Graphical User Interface (GUI) capabilities, referred to as Surface Water Identification and Forecasting Tool (SWIFT). SWIFT allows ranchers, and land managers to access near real-time observations of surface water extents, thereby greatly reducing the substantial time and cost required to monitor stock ponds through *in situ* observations. By selecting an area of interest using drop-down tabs for the following options—state, national forest, ranger district, and grazing allotment—users can assess current water extents relative to historical extents, as well as export multiple datasets for comparison between allotments. This tool is meant to supplement field monitoring and will reduce the time and cost required by land managers and ranchers to physically drive to check remote stock ponds. By efficiently accessing both historical data and current conditions for hundreds of stock ponds and other water features, SWIFT will enable partners to develop adaptive management strategies in years to come.

The temporal cadence of observations within the tool is dependent on the temporal resolution of remote sensing datasets in addition to the lag time between image capture and image availability through GEE (~1-2 days). Sentinel-2's temporal resolution (5 days) is significantly higher than that of Sentinel-1(12 days) or Landsat 8 (16 days). The most recent image capture date is displayed to the user upon image classification.

4.1.2 Time Series Maps

Figure 4 displays the average monthly total surface area of water in the study area since 2013 using the image processing workflow presented here, as well as the monthly moving mean precipitation for the study area from gridMET. GridMET is a dataset of daily high-spatial resolution (~4-km, 1/24th degree) surface meteorological data covering the contiguous US from 1979 to the present, accessible through GEE and Climate Engine (Abatzoglou, 2013). Our findings show that the method captures both seasonal and interannual variations in regional water surface area. We observed the maximum surface water extent in the study area of ~220 km^2 in the winter of 2021. Other notable peaks in water extent occurred during the spring of 2020 and summer of 2018.

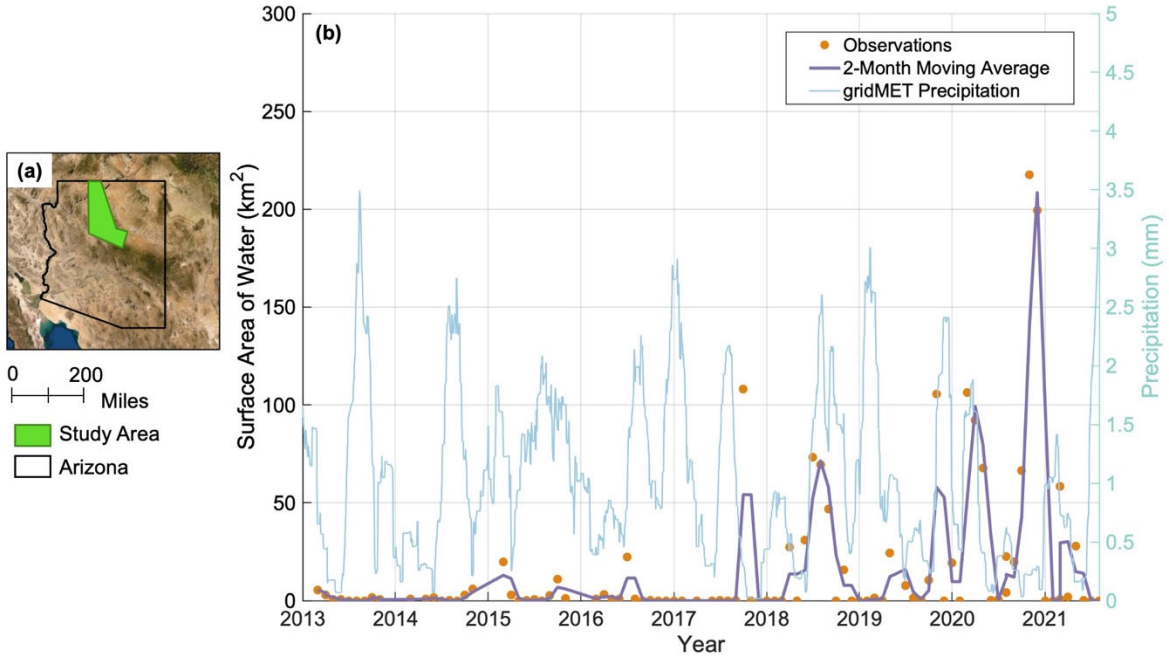

Figure 4. (a) Map of the study area with the Arizona state borders marked. (b) Time series of average monthly total surface areas of water in the study area since March 2013 with the 2-month moving average (purple). The monthly moving average precipitation for the study area from gridMET (Abatzoglou, 2013) is shown along the right y-axis (blue).

In addition to the overall trends in surface water extent, we analyzed the cross-correlation with the regional precipitation during the study period (Figure B1). We found a maximum cross-correlation value for a lag time of –1 month. We interpret this to show that increases in surface water throughout the study area occur most often after one month of increased precipitation. We also note particularly low surface water extents (less than 50 km^2) and cross-correlation values before 2018 despite persistent precipitation. These low values may be due to limited satellite observations. Sentinel products are not available through GEE for all dates, which may decrease the spatial coverage of observations and increase the likelihood of masked pixels due to cloud cover in Landsat 8 imagery.

To further analyze regional trends throughout Arizona in recent years, we computed the average monthly total surface area of water in each National Forest in Arizona (Figure B1). Here, we see that the Coronado, Coconino, and Apache-Sitgreaves National Forests contribute the majority of total water area throughout the state. In contrast, the Tonto, Prescott, and Kaibab National Forests show consistently low water extents throughout the study period with respect to other forests, with some notable increases in water extent in the Tonto National Forest in 2021. It should be noted that not all Arizona National Forests lie within the designated study area; therefore, the total surface water extents in the study area and National Forests are not directly relatable.

4.1.3 Accuracy Assessment, Error, and Uncertainties

Wet, muddy, or moist surfaces can increase the likelihood of commission errors due to increased backscatter in Sentinel-1 imagery, or a spectral signature similar to that of surface water bodies in optical imagery. Sentinel-1 classified imagery seems to overestimate water surface areas during wetter seasons in the region (Figure B2), which may bias estimates of surface water extent in the winter months when optical imagery is not usable. To combat these potential errors or decreased spatial coverage due to cloud cover, Sentinel-1 imagery has shown to successfully capture water features which were otherwise filtered out by clouds in optical imagery captured the same week (Figure 5, Figure B2).

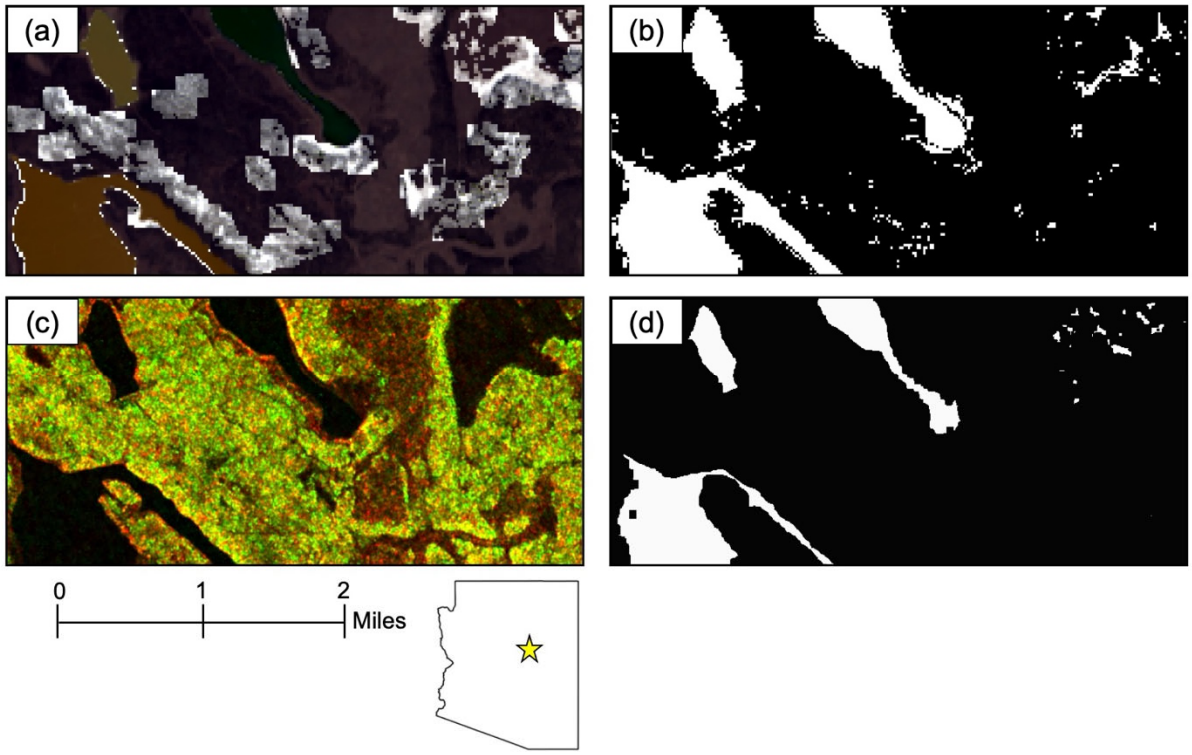

Figure 5 (a) Pre-processed true color mosaic of optical (Landsat 8 and Sentinel-2) imagery. (b) Classified optical imagery. (c) Pre-processed, false color Sentinel-1 imagery displayed using the VV and VH polarization bands. (d) Classified Sentinel-1 imagery. For classified imagery (b and d), black represents non-water points and white represents classified surface water. All images were captured in January 2018. The regional map (bottom) shows the zoomed in area located in Arizona shown in panels (a) - (d) represented by the yellow star.

We also observed evidence of decreased classification accuracy due to turbid water surfaces and local variations in surface roughness. This was particularly an issue observed in classified Sentinel-1 image mosaics, as this classification model relies on the total returns reaching the antenna, as opposed to the optical signature at varying spectral wavelengths. To minimize these impacts, we implemented the boxcar smoothing algorithm and wind masking for Sentinel-1 imagery as well as the HAND filter applied to image mosaics to decrease noise associated with turbid water surfaces and anomalies on ridge lines and other topographic features, for example. Although several steps were taken to mitigate the effects of vegetation cover, some water bodies may be located beneath vegetation, particularly in the more densely vegetated northern region of the study area. Remote observations of these water bodies may therefore not be detected here, potentially leading to underestimated surface water extents.

Additionally, the exact quantities of the surface water extent time series maps may be subject to errors associated with decreased geographic coverage due to the various filters and masking algorithms. Particularly because only Landsat 8 is available through GEE before 2017, the 2013-2017 water extents may be limited by cloud masking. We suggest quantifying the total masked area in each image mosaic to increase the confidence and contextual information for the time series maps. The accuracy assessment of our work is also limited by a lack of *in situ* observations in the region to validate our classifications (Table 2). We suggest the implementation of on-site observation systems at several accessible stock pond sites throughout the region to validate and refine indices across a variety of land cover conditions in future work.

Table 2

Summary of method accuracy assessment. Overall accuracy and Kappa Coefficient and confusion matrices for classified optical imagery (Landsat 8 & Sentinel-2) and classified SAR imagery (Sentinel-1).

	Landsat 8 & Sentinel-2	**Sentinel-1**
Overall Accuracy	93%	88%
Kappa Coefficient	88%	76%
Confusion Matrices		

	Water	**Non-water**
Water	34	2
Non-water	2	27

	Water	**Non-water**
Water	27	4
Non-water	2	18

4.2 Future Work

Successful results of this research present the opportunity to expand EO-based small water body monitoring into other western states facing similar drought conditions like Utah, Idaho, and California. Future projects should include stock ponds on additional ranches, national forests, Bureau of Land Management districts, and state lands. Furthermore, in 2022, two new NASA missions will be launching. The NASA-ISRO SAR (NISAR) is a joint mission between NASA and the Indian Space Research Organization (ISRO) to produce a SAR to help understand the Earth's changing ecosystems. NISAR, launching in early 2023, will provide a temporal resolution of twelve days. The Surface Water and Ocean Topography (SWOT) mission (November 2022) will provide a means to monitor and track Earth's water resources. These two missions warrant further research of possible applications in small water body detection and extent.

SWIFT may have additional applications other than monitoring water surface extent within grazing allotments. For example, wildfire operations rely heavily upon aerial resources to support ground crews. Helicopters supply water to the fire line by hauling water from the closest water body. Fire managers currently rely on known water body locations or by scouting missions. SWIFT could aid fire management through detecting water bodies capable of supporting air operations.

5. Conclusions

The results from this study involving the analysis of spectral band indices (Automated Water Extraction Index, Modified Normalized Difference Water Index, and Tasseled Cap-wetness index) and the incidence angle, VV, and VH polarization bands for synthetic aperture radar imagery for detecting surface water bodies showed that the data products from Landsat 8, Sentinel-2, and the Sentinel-1 are sufficient to determine the extents of stock ponds in the study area with overall accuracies of 88-93%.

The indices employed here have been selected based on their ability to efficiently and accurately identify surface water features in previous studies. This study provides a detailed time-series analysis of stock pond water extents. Similarly, the development of an accessible tool for future surface water extent change detection will not only complement in-situ observation of stock pond measurements currently in use, but it will also empower our partners to monitor in near real-time (on a weekly basis as acquired satellite data becomes available) their stock pond water availability. This represents a novel approach in monitoring surface water extents of remote stock ponds in this region, and this will bring about sustainable and efficient land and livestock management practices.

In closing, complementary to the adopted method for this study, future work might incorporate data from the soon-to-be-launched NASA missions, including NISAR and SWOT, which will enable expansion of the stock pond time series analysis maps and the potential for more frequent observations implemented into the monitoring tool for use in the study area and other Southwestern region frontiers.

6. Acknowledgments

We would like to thank several contributors to this work, including science advisors: Keith Weber (GIS Training and Research Center, Idaho State University) and Seungbum Kim (Radar Remote Sensing, NASA Jet Propulsion Laboratory); project partners: Iric Burden (Range Program, Kaibab National Forest, USFS), Steve Cassady (Arizona Department of Game and Fish), Lisa Bolten (Diablo Trust), Kit Metzger (The Flying M Ranch), and Bob Prosser (The Bar T Bar Ranch); and collaborator: Matt Reeves (Rocky Mountain Research Center, USFS). Additional thanks to Brandy Nisbet-Wilcox (NASA DEVELOP Fellow), Rebekke Muench (NASA SERVIR), as well as Stephanie Granger and Forrest Melton (NASA Western Water Applications Office).

This material contains modified Copernicus Sentinel data (2014-2021), processed by ESA.

Any opinions, findings, and conclusions or recommendations expressed in this material are those of the author(s) and do not necessarily reflect the views of the National Aeronautics and Space Administration.

This material is based upon work remotely supported by NASA through contract NNL16AA05C.

7. Glossary

Automated Water Extraction Index, shadow-corrected (AWEIsh) – Index estimating surface water content using the blue, green, near infrared, and shortwave infrared surface reflectance.
Backscatter – Energy reflected back from the terrain toward the radar system
Earth observations (EO) – Satellites and sensors that collect information about the Earth's physical, chemical, and biological systems over space and time
Google Earth Engine (GEE) – Cloud computing platform combining satellite imagery and geospatial datasets of Earth's surface
Graphical User Interface (GUI) – Visual components of a computer software utilized by users
Indian Space Research Organization (ISRO) – National space agency of India
Landsat 8 Operational Land Imager (OLI) – Imaging instrument aboard the Landsat 8 satellite. OLI can measure visible, near-infrared, and shortwave infrared wavelengths.
Light Detection and Ranging (LiDAR) – Remote sensing method providing accurate elevation data by emitting laser pulses and measuring their return.
Modified Normalized Difference Water Index (MNDWI) – Index estimating surface water content of vegetation using middle infrared band from satellite missions

NASA-ISRO SAR (NISAR) – Joint mission between NASA and the Indian Space Research Organization (ISRO) to produce fine-resolution radar images and measure Earth's changing ecosystems, dynamic surfaces, and ice masses providing information about biomass, natural hazards, sea level rise, and groundwater.
NASA RECOVER Western US Geodatabase – Funded by NASA, maintained by the Idaho State University GIS Training and Research Center
Near-infrared (NIR) – A subset of the infrared portion of the electromagnetic spectrum ranging from 750-2500 nm, often used for investigating surface plant and soil cover in remote sensing applications.
Normalized Difference Vegetation Index (NDVI) – Index used to assess the presence of live green vegetation using near-infrared and red surface reflectance
Normalized Difference Water Index (NDWI) – Index estimating surface water content of vegetation using near-infrared and shortwave infrared surface reflectance
Remote Sensing – Detection, measurement, and acquisition of Earth's surface characteristics using sensors on satellites, and aircraft
Sentinel-1 C-Band Synthetic Aperture Radar (C-SAR) – European Space Agency constellation consisting of two satellites, Sentinel-1A and Sentinel-1B, each carrying a C-SAR instrument
Sentinel-2 MultiSpectral Instrument (MSI) – Mission using wide-swath, high-resolution, multi-spectral imaging to monitor vegetation, soil, and inland and coastal water cover
Shortwave Infrared (SWIR) – A subset of the infrared portion of the electromagnetic spectrum ranging from 1400-3000 nm, able to discriminate between clouds, snow, and ice.
Surface Water and Ocean Topography (SWOT) – Mission to produce high-resolution 2D observations of sea-surface height using SAR radar techniques that combine different wavelengths.
Surface Water Identification and Forecasting Tool (SWIFT) – Tool developed through this project that detects water extent change on Earth's surface
Synthetic Aperture Radar (SAR) – Instrument operating under all-weather and all day and night conditions, using the Doppler shift to monitor beams returning to the sensor
Tasseled Cap Wetness (TCW) – Index contrasting visible and near-infrared bands with shortwave infrared bands
US Forest Service (USFS)
VH – Cross-polarization band used in Sentinel-1 C-SAR imagery
VV – Co-polarization band used in Sentinel-1 C-SAR imagery

8. References

Abatzoglou, J. T. (2013). Development of gridded surface meteorological data for ecological applications and modelling. *Int. J. Climatol.*, *33*, 121–131.

Abrams, R. H. (2010). Correcting mismatched authorities: Erecting a new water federalism. *Natural Resources & Environment*, *25*, 22.

Alsdorf, D. E., Rodríguez, E., and Lettenmaier, D. P. (2007). Measuring surface water from space, *Reviews of geophysics.*, 45, RG2002. https://doi.org/10.1029/2006RG000197

Archer, S. R., & Predick, K. I. (2008). Climate change and ecosystems of the southwestern United States. *Rangelands*, *30*(3), 23–28. https://doi.org/10.2111/1551-501X(2008)30[23:CCAEOT]2.0.CO;2

Baig, M. H. A., Zhang, L., Dong, J., Li, Y., She, X., & Qingxi, T. (2014). Water mapping through Universal Pattern Decomposition Method and Tasseled Cap Transformation. *2014 IEEE Geoscience and Remote Sensing Symposium*, 4758–4760. https://doi.org/10.1109/IGARSS.2014.6947557

Bioresita, F., Puissant, A., Stumpf, A., & Malet, J.-P. (2018). A method for automatic and rapid mapping of water surfaces from Sentinel-1 imagery. *Remote Sensing*, *10*(2), 217. https://doi.org/10.3390/rs10020217

Copernicus Sentinel data (2021). Retrieved from Google Earth Engine 25 June 2021, processed by ESA.

DeVries, B., Huang, C., Armston, J., Huang, W., Jones, J. W., & Lang, M. W. (2020). Rapid and robust monitoring of flood events using Sentinel-1 and Landsat data on the Google Earth Engine. *Remote Sensing of Environment*, *240*, 111664. https://doi.org/10.1016/j.rse.2020.111664

Feyisa, G. L., Meilby, H., Fensholt, R., & Proud, S. R. (2014). Automated Water Extraction Index: A new technique for surface water mapping using Landsat imagery. *Remote Sensing of Environment*, *140*, 23–35. https://doi.org/10.1016/j.rse.2013.08.029

Fisher, A., Flood, N., & Danaher, T. (2016). Comparing Landsat water index methods for automated water classification in eastern Australia. *Remote Sensing of Environment*, *175*, 167–182. https://doi.org/10.1016/j.rse.2015.12.055

Garousi-Nejad, I., Tarboton, D. G., Aboutalebi, M., & Torres-Rua, A. F. (2019). Terrain analysis enhancements to the height above nearest drainage flood inundation mapping method. *Water Resources Research*, *55*(10), 7983–8009. https://doi.org/10.1029/2019WR024837

Gulácsi, A., & Kovács, F. (2020). Sentinel-1-imagery-based high-resolution water cover detection on wetlands, aided by Google Earth Engine. *Remote Sensing*, *12*(10), 1614. https://doi.org/10.3390/rs12101614

Hamdani, N., & Baali, A. (2019). Height Above Nearest Drainage (HAND) model coupled with lineament mapping for delineating groundwater potential areas (GPA). *Groundwater for Sustainable Development*, *9*, 100256. https://doi.org/10.1016/j.gsd.2019.100256

Herndon, K., Muench, R., Cherrington, E., & Griffin, R. (2020). An assessment of surface water detection methods for water resource management in the Nigerien Sahel. *Sensors*, *20*(2), 431. https://doi.org/10.3390/s20020431

Hoekman, D. H., & Reiche, J. (2015). Multi-model radiometric slope correction of SAR images of complex terrain using a two-stage semi-empirical approach. *Remote Sensing of Environment*, *156*, 1–10. https://doi.org/10.1016/j.rse.2014.08.037

Meehan, M. A., O'Brien, P. L., Hecker, G. A., & Printz, J. L. (2021). Integrating rangeland health and stream stability in assessments of rangeland watersheds. *Rangeland Ecology & Management*, *75*, 104-111. https://doi.org/10.1016/j.rama.2020.12.005

Mishra, V., Limaye, A. S., Muench, R. E., Cherrington, E. A., & Markert, K. N. (2020). Evaluating the performance of high-resolution satellite imagery in detecting ephemeral water bodies over West Africa. *International Journal of Applied Earth Observation and Geoinformation*, *93*, 102218. https://doi.org/10.1016/j.jag.2020.102218

Mullissa, A., Vollrath, A., Odongo-Braun, C., Slagter, Balling, J., Gou, Y., Gorelick, N., & Reiche, J. (2021). Sentinel-1 SAR backscatter analysis ready data preparation in Google Earth Engine. *Remote Sensing*, 13(10), 1954. https://doi.org/10.3390/rs13101954

National Centers for Environmental Information (NCEI). (2021a, August). *Climate at a Glance | Temperature | Coconino County | June-August | 1971-2021*. https://www.ncdc.noaa.gov/cag/county/time-series/AZ-005/tavg/3/8/1971-2021?base_prd=true&begbaseyear=1971&endbaseyear=2021

National Centers for Environmental Information (NCEI). (2021b, August). *Climate at a Glance | Temperature | Yavapai County | June-August | 1971-2021*. https://www.ncdc.noaa.gov/cag/county/time-series/AZ-025/tavg/3/8/1971-2021?base_prd=true&begbaseyear=1971&endbaseyear=2021

National Centers for Environmental Information (NCEI). (2021c, August). *Climate at a Glance | Precipitation | Coconino County | June-August | 1971-2021*. https://www.ncdc.noaa.gov/cag/county/time-series/AZ-005/pcp/3/8/1971-2021?base_prd=true&begbaseyear=1971&endbaseyear=2021

National Centers for Environmental Information (NCEI). (2021d, August). *Climate at a Glance | Precipitation | Yavapai County | June-August | 1971-2021*. https://www.ncdc.noaa.gov/cag/county/time-series/AZ-025/pcp/3/8/1971-2021?base_prd=true&begbaseyear=1971&endbaseyear=2021

Nguyen, U. N. T., Pham, L. T. H., & Dang, T. D. (2019). An automatic water detection approach using Landsat 8 OLI and Google Earth Engine cloud computing to map lakes and reservoirs in New Zealand. *Environmental Monitoring and Assessment*, *191*(4), 1–12. https://doi.org/10.1007/s10661-019-7355-x

Nobre, A. D., Cuartas, L. A., Hodnett, M., Rennó, C. D., Rodrigues, G., Silveira, A., Waterloo, M., & Saleska, S. (2011). Height Above the Nearest Drainage – a hydrologically relevant new terrain model. *Journal of Hydrology*, *404*(1), 13–29. https://doi.org/10.1016/j.jhydrol.2011.03.051

Ovakoglou, G., Cherif, I., Alexandridis, T., Pantazi, X., Tamouridou, A., Moshou, D., Tseni, X., Raptis, I., Kalaitzopoulou, S., & Mourelatos, S. (2021). Automatic detection of surface-water bodies from Sentinel-1 images for effective mosquito larvae control. *Journal of Applied Remote Sensing, 15*(1), 014507. https://doi.org/10.1117/1.JRS.15.014507

Saha, S., et al. 2011, updated daily. NCEP Climate Forecast System Version 2 (CFSv2) 6-hourly Products. Research Data Archive at the National Center for Atmospheric Research, Computational and Information Systems Laboratory. https://doi.org/10.5065/D61C1TXF. Accessed 09 08 2021.

Soti, V., Tran, A., Bailly, J.-S., Puech, C., Seen, D. L., & Bégué, A. (2009). Assessing optical earth observation systems for mapping and monitoring temporary ponds in arid areas. *International Journal of Applied Earth Observation and Geoinformation*, *11*(5), 344–351. https://doi.org/10.1016/j.jag.2009.05.005

Xu, H. (2006). Modification of Normalized Difference Water Index (NDWI) to enhance open water features in remotely sensed imagery. *International Journal of Remote Sensing*, *27*, 3025–3033. https://doi.org/10.1080/01431160600589179

Yamazaki, D., Ikeshima, D., Sosa, J., Bates, P.D., Allen, G.H., & Pavelsky, T.M. (2019). MERIT Hydro: A high-resolution global hydrography map based on latest topography datasets. *Water Resources Research*, *55*, 5053–5073. https://doi.org/10.1029/2019WR024873

Zhu, Z., & Woodcock, C. E. (2012). Object-based cloud and cloud shadow detection in Landsat imagery. *Remote Sensing of Environment*, *118*, 83–94. https://doi.org/10.1016/j.rse.2011.10.028

Zhu, Z., Wang, S., & Woodcock, C. E. (2015). Improvement and expansion of the Fmask algorithm: Cloud, cloud shadow, and snow detection for Landsats 4–7, 8, and Sentinel 2 images. *Remote Sensing of Environment*, *159*, 269–277. https://doi.org/10.1016/j.rse.2014.12.014

9. Appendices

Appendix A

Table A1
Summary of Datasets Used

Satellite-Derived Data Product	**Available Temporal Coverage**	**Spatial Resolution**	**Parameters**
Landsat 8 OLI Surface Reflectance Tier 2	February 2013 – July 2021	30 meters	Modified Normalized Difference Water Index (MNDWI) Automated Water Extraction Index, shadow-corrected ($AWEI_{sh}$) Tasseled-Cap Wetness (TCW) Normalized Difference Vegetation Index (NDVI)
Sentinel -1 C-SAR Ground Range Detected	April 2014 – July 2021	10 meters	Co-polarization (VV) and cross polarization (VH) bands Instrument angle
Sentinel-2 MSI, Level 2-A	June 2015 – July 2021	10 meters (B,G,R, NIR) 20 meters (SWIR1, SWIR2)	Modified Normalized Difference Water Index (MNDWI) Automated Water Extraction Index, shadow-corrected ($AWEI_{sh}$) Tasseled-Cap Wetness (TCW) Normalized Difference Vegetation Index (NDVI)
Maxar High-Resolution Imagery*	January 2015 – December 2020	0.5 meter	Digitized "water" and "non-water" points used for training the classification model and accuracy assessment
USFS and Bar T Bar Ranch stock ponds points	N/A		Study area, points of interest

The "*" indicates commercial imagery not shared with partners or end users

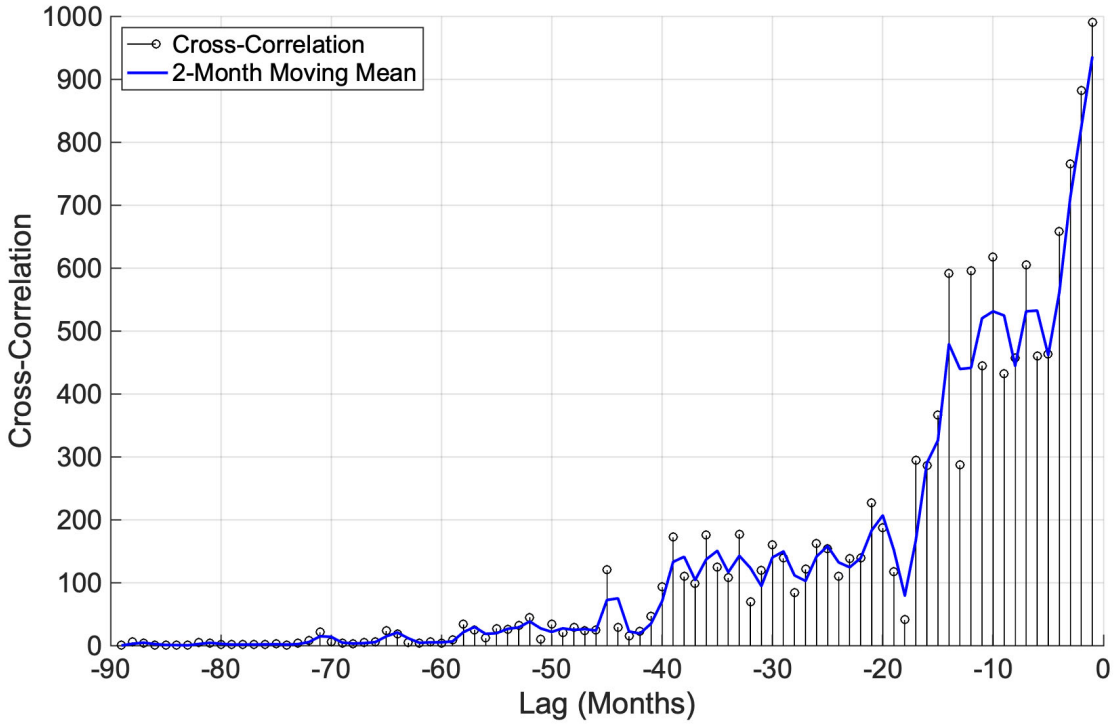

Figure B1. Plot of cross-correlation between the precipitation and surface water extent in the study area, with the 2-month lag moving mean of the cross-correlation represented by the blue line.

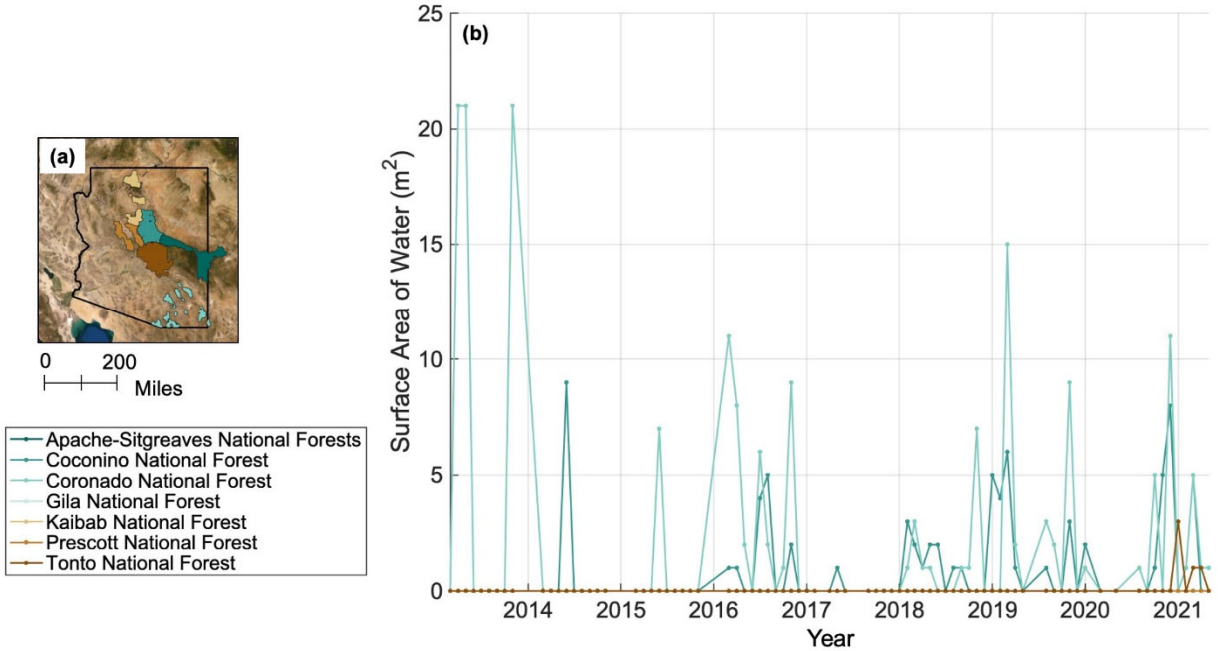

Figure B2 (a) Map of National Forests located in Arizona with state borders marked. (b) Time series of average monthly total surface areas of water in each National Forest since March 2013.